ACS APPLIED MATERIALS & INTERFACES

Letter

www.acsami.org

Plasma-Assisted Synthesis of High-Mobility Atomically Layered Violet Phosphorus

Hsu-Sheng Tsai,[†] Chih-Chung Lai,[†] Ching-Hung Hsiao,[†] Henry Medina,[†] Teng-Yu Su,[†] Hao Ouyang,[†] Tai-Hsiang Chen,[‡] Jenq-Horng Liang,*[,‡,§] and Yu-Lun Chueh*[,†]

[†]Department of Material Science and Engineering, [‡]Institute of Nuclear Engineering and Science, and [§]Department of Engineering and System Science, National Tsing Hua University, Hsinchu 30013, Taiwan, R.O.C.

Supporting Information

ABSTRACT: Two-dimensional layered materials such as graphene, transition metal dichalcogenides, and black phosphorus have demonstrated outstanding properties due to electron confinement as the thickness is reduced to atomic scale. Among the phosphorus allotropes, black phosphorus, and violet phosphorus possess layer structure with the potential to be scaled down to atomically thin film. For the first time, the plasma-assisted synthesis of atomically layered violet phosphorus has been achieved. Material characterization supports the formation of violet phosphorus/InN over InP substrate where the layer structure of violet phosphorus is clearly observed. The identification of the crystal structure and lattice constant ratifies the formation of violet phosphorus indeed. The critical concept of this synthesis method is the selective reaction induced by different variations of Gibbs free energy (ΔG) of reactions. Besides, the Hall mobility of the violet phosphorus on the InP substrate greatly increases over the theoretical values of InP bulk material without much reduction in the carrier concentration, suggesting that the mobility enhancement results from the violet phosphorus layers. Furthermore, this study demonstrates a low-cost technique with high compatibility to synthesize the high-mobility atomically layered violet phosphorus and open the space for the study of the fundamental properties of this intriguing material as a new member of the fast growing family of 2D crystals.

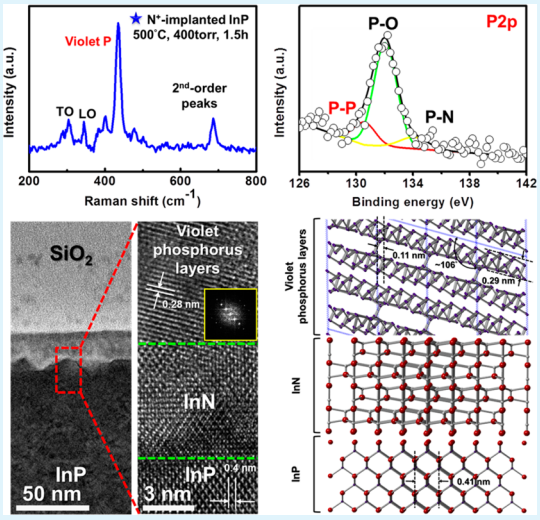

KEYWORDS: *plasma, violet phosphorus, mobility, selective reaction, two-dimensional materials*

The field of two-dimensional (2D) materials was pioneered by the advent of graphene.[1] The zero-band gap restricts its development in switching devices despite its extraordinary physical properties such as ultrahigh carrier mobility (>250,000 $cm^2/(V\ s)$)[2] and transparency (~97%).[3] Recently, transition metal dichalcogenides (TMDs), that includes MoS_2, $MoSe_2$, WS_2, and so on, have become the most popular compound materials for researches.[4−6] In addition to the existence of band gap, the most attractive characteristic of TMDs is the transformation from indirect to direct band gap as the monolayer is reached.[6] Up to now, chemical vapor deposition (CVD)[7] is the only method for obtaining TMDs films besides mechanical exfoliation. Nevertheless, large-scale continuous TMDs films directly synthesized on particular substrates with or without transfer step, remains a major challenge.

Phosphorene, which is a single-atomic layer of black phosphorus, is the new and hot single-elemental material with outstanding impact in the area of 2D materials. In fact, the most common allotropes of phosphorus are the red and white phosphorus, whereas the black phosphorus is not easily accessible and its synthesis requires complex processing. Black phosphorus is indeed a potential candidate for switching device application since its band gap can be changed from ~0.34 eV to ~2 eV once the scale is down to single layer.[8] Furthermore, the carrier mobility would attain to ~1000 $cm^2/(V\ s)$, which is much higher than that of TMDs, as well as on−off current ratio of more than 5 orders magnitude.[9] Even so, most of researches rely on exfoliation of black phosphorus nanosheets for fabrication of transistors in order to demonstrate its outstanding electrical properties.[9] Concerning the large scale synthesis of black phosphorus, the only method reported by Li et al.[8] employed a cubic-anvil-type apparatus to heat red phosphorus on SiO_2-capped Si substrate at 1000 °C under 10 kbar for the formation of the black allotrope. The condition of this process is quite complex and difficult to accomplish, especially due to the high working pressure. T. Nilges et al.[10] have announced a synthesis method of black phosphorus at standard pressure. However, it is actually not a

Received: May 1, 2015
Accepted: June 12, 2015
Published: June 12, 2015

DOI: 10.1021/acsami.5b03803
ACS Appl. Mater. Interfaces 2015, 7, 13723−13727

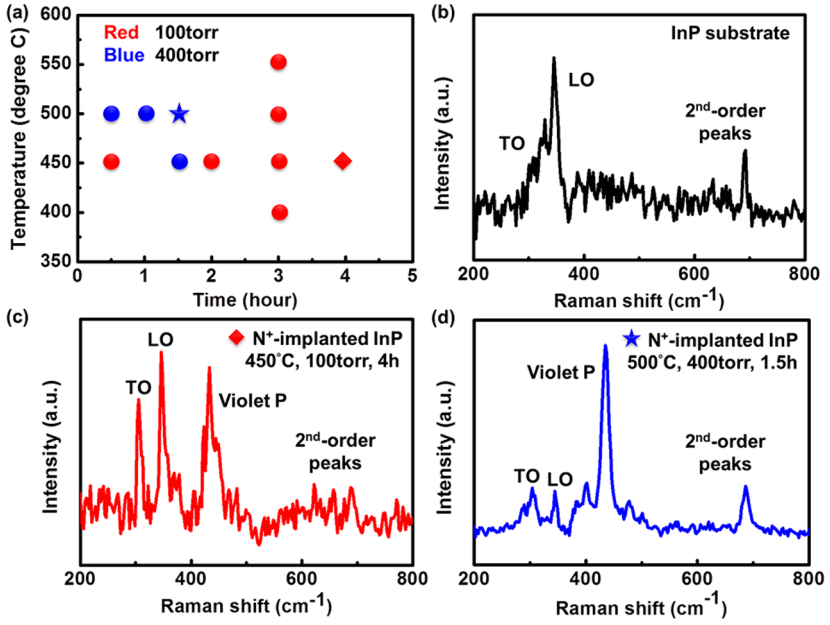

Figure 1. (a) Condition window plot for atomically layered violet phosphorus synthesis via the plasma-assisted process. (b) Spectrum of pristine InP substrate. (c) Spectrum of N^+-implanted InP after 450 °C annealing under 100 Torr for 4 h. (d) Spectrum of N^+-implanted InP after 500 °C annealing under 400 Torr for 1.5 h.

process at standard pressure since the powder of red phosphorus and the solid catalyst (SnI_4) with low boiling point (~364 °C) are sealed into a silica ampule (length 50 mm, inner diameter 8 mm) during a thermal treatment (550−650 °C). As can be imagined, the vapor pressure inside the silica ampule must be quite high. Furthermore, the large scale black phosphorus cannot be achieved by this method, and the purity of it should not be high enough for applications because of the residual catalyst.

A simple plasma-assisted process for direct synthesis of few-layered graphene on 4H-SiC substrate has been previously developed in our laboratory.[11] In this work, we expand this technique for the synthesis of the atomically layered violet phosphorus on the InP substrate. In fact, the violet phosphorus is another allotrope of phosphorus, which is expected to display semiconducting behavior with band gap of 1.5 eV.[12] It also possesses quasi-2D layered structure that belongs to the monoclinic crystal constructed by 21 phosphorus atoms in each unit cell.[13] In contrast to black phosphorus, the violet phosphorus does not require such a high working pressure and can be formed by annealing red phosphorus in a sealed tube at 530 °C.[14,15] It is also suggested that Hittorf discovered violet phosphorus upon recrystallization from molten lead.[14,15] Therefore, it is also named as Hittorf's phosphorus. In this study, it is worth mentioning that the atomically layered violet phosphorus with high carrier mobility on the InP substrate was obtained by our process (see the Supporting Information).

RESULTS AND DISCUSSION

The condition window plot of the plasma-assisted process shown in Figure 1a represents the course of process optimization. After N_2 plasma exposure, we initially annealed the InP samples with varying temperatures of 400 to 550 °C in 50 °C steps for 3 h under 100 and 400 Torr. The surface of samples annealed above 500 °C were with metallic cluster and became much rougher, implying that the indium metal decomposed on the surface. Based on our previous work,[11] we suggest that InN might be formed during annealing process since the nitrogen ions introduced by plasma tend to preferentially react with indium; and, the phosphorus would be condensed onto the surface simultaneously. However, InN is quite unstable at temperatures above 500 °C because of its low dissociation temperature and high equilibrium nitrogen vapor pressure over the InN film.[16] Hence, we first set the annealing temperature at 450 °C under 100 Torr and gradually changed the annealing time from 0.5 to 4 h. The red diamond in Figure 1a shows the best condition among all of the cases under 100 Torr. As can be seen in the Raman spectra (Figure 1b, c), a series of peaks attributed to violet phosphorus appear over the range of 360−480 cm^{-1} after the N_2 plasma exposure followed by annealing at 450 °C under 100 Torr for 4 h, in addition to the intrinsic peaks of InP. These peaks are divided into three parts including extended (430−480 cm^{-1}), longitudinal (~420 cm^{-1}), and transverse (360−400 cm^{-1}) breathing modes.[17] On the other hand, the transverse optical (TO) mode of InP becomes much sharper after the annealing process since the lattice damage induced by plasma bombardment is too serious to be totally recovered by annealing below 700 °C.[18] Afterward, we attempted to increase the working pressure during annealing in order to prevent decomposition of InN, which may obstruct the condensation of phosphorus and destroy the as-formed phosphorus layers. Besides the lower working pressure during the annealing process, we supposed that the decomposition of InN would be caused by either higher annealing temperature or longer annealing time. To tackle it, the working pressure was further increased to 400 Torr; meanwhile, the annealing period at 450 °C was reduced to 1.5 h. Unfortunately, the Raman result similar to that of Figure 1c could not be stably repeated. A great result (Figure 1d), which is better and more stable than that of Figure 1c, was obtained by slightly increasing the annealing temperature to 500 °C under 400 Torr for 1.5 h. The intensity of the longitudinal breathing mode of the violet phosphorus is nearly 4 times stronger than that of InP intrinsic peaks, indicating that the

DOI: 10.1021/acsami.5b03803
ACS Appl. Mater. Interfaces 2015, 7, 13723−13727

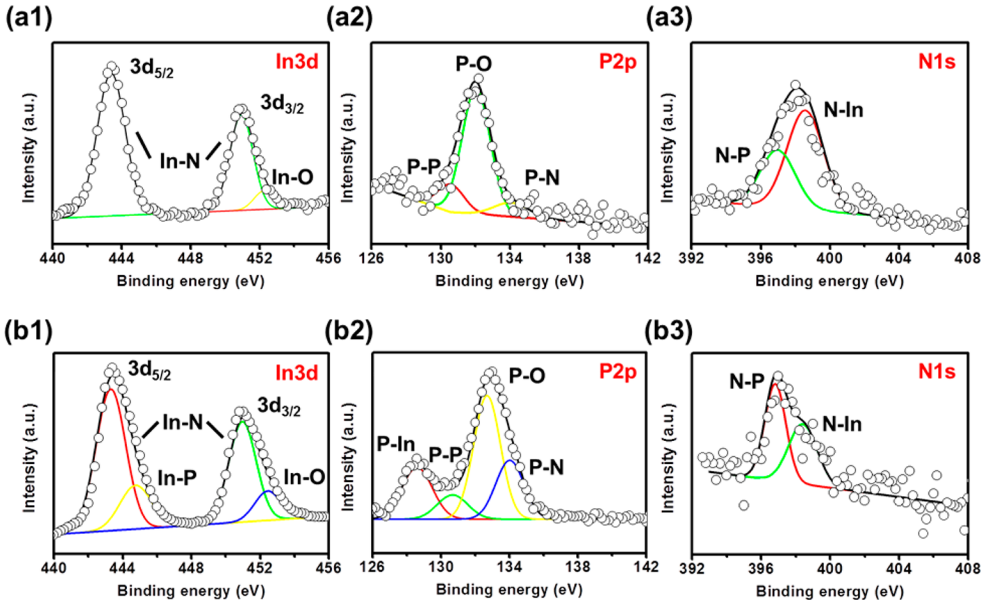

Figure 2. (a) In 3d (a1), P 2p (a2), and N 1s (a3) spectra of the surface. (b) In 3d (b1), P 2p (b2), and N 1s (b3) spectra of 10 nm depth below the surface.

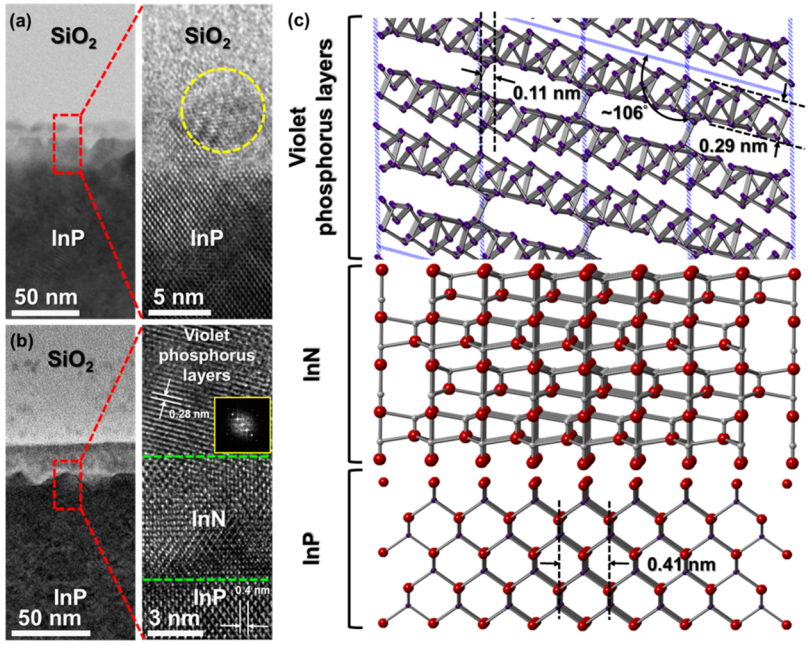

Figure 3. (a) TEM images of N^+-implanted InP after 450 °C annealing under 100 Torr for 4 h. (b) TEM images of N^+-implanted InP after 500 °C annealing under 400 Torr for 1.5 h. (c) Atomic model of violet phosphorus/InN/InP layer structure. Inset: diffraction pattern of violet phosphorus.

crystallinity is largely enhanced. We also tried to further reduce the annealing time of this condition, but the Raman peaks of violet phosphorus could not be apparently observed. According to the Raman results, we initially suggest that the violet phosphorus was successfully synthesized on the surface of InP by the plasma-assisted process. Although the synthesis condition is quite narrow, the process has been optimized.

Further surface analysis was implemented to prove the synthesis mechanism of the violet phosphorus. The results of X-ray photoemission spectroscopy (XPS) are shown in Figure 2. Among all the spectra, the oxygen-related peaks including In−O (~452.5 eV) and P−O (~132.2 eV) are inevitably caused by the atmosphere. At the surface region, the intense In−N peak which splits into $3d_{5/2}$ (~443.4 eV) and $3d_{3/2}$ (~450.9 eV) can be directly observed in the In 3d spectrum (Figure 2a1), implying that InN might be formed after the annealing process. In the P 2p spectrum (Figure 2a2), the weak P−P and P−N bonding signals overlapped with that of P−O bonding are located at ~130.5 eV and ~134.2 eV, respectively. It indicates that the single-elemental phosphorus structure doped with nitrogen might be also created. Figure 2a3 shows the nitrogen-related peak that comprises N−P (~396.7 eV) and N−In (~398.4 eV) subpeaks caused by the plasma immersion. At the 10 nm-depth region, the bonding signals originated from the InP substrate emerge in the spectra as shown in Figure 2b1, b2. The nitrogen-related peak is still

DOI: 10.1021/acsami.5b03803
ACS Appl. Mater. Interfaces 2015, 7, 13723−13727

observed in the N 1s spectrum (Figure 2b3) but the intensity is actually weaker. This analytical result confirms that a phosphorus thin film was synthesized on InP substrate indeed. In other words, the indium should be reacted with nitrogen ions to form InN after the annealing process.

Eventually, the truly atomic structure would be monitored by transmission electron microscope (TEM). The SiO_2 layer was deposited by electron beam evaporator to protect the thin film from damage for TEM sample prepared by focus ion beam (FIB). TEM images of the violet phosphorus on the InP substrate synthesized by low and high pressure annealing conditions are shown in panels a and b in Figure 3, respectively. The low-magnification image of the low pressure case (100 Torr) exhibits an indistinct layer, which might be the violet phosphorus, on the surface of the InP substrate. There is a bulge with the violet phosphorus layers surrounded by the circular dash line in high-magnification image of Figure 3a. Obviously, this noncontinuously interrupted structure most likely resulted from the decomposition of the InN because the working pressure of annealing was too low to suppress it. Therefore, the deteriorated crystal structure of violet phosphorus corresponds to the relatively weaker Raman peak in Figure 1c. Oppositely, a ~20 nm thick violet phosphorus film is clearly capped on the surface of InP as shown in the low-magnification image of Figure 3b. The layer structure under high magnification is totally consistent with our anticipation. The (110) interplanar distance (~0.4 nm) of InP is in agreement with the theoretical one as labeled in Figure 3c. The middle InN layer with worse crystallinity comes from the reaction between nitrogen ions and indium in defective InP at the moderate temperature. It may be the reason that the Raman peaks of InN could not be detected. The atomically layered phosphorus with layer spacing of ~0.28 nm stacked on the top of the InN layer (Figure 3c) shows good agreement with the theoretical layer spacing expected for the violet phosphorus (~0.29 nm).[13] The inset of Figure 3b shows the diffraction pattern of the violet phosphorus structure processed by Fast Fourier Transform (FFT). The lattice parameters such as horizontal spacing and layer spacing estimated from the reciprocal vectors are 0.111 and 0.278 nm, respectively (Figure S1 in the Supporting Information). Moreover, the phosphorus atoms were condensed onto the surface and arranged into the violet phosphorus structure along [001] direction. The crystal structure of the violet phosphorus belongs to the monoclinic system whose β angle is ~106°.[13] Hence the violet phosphorus layers are stacked with ~106° toward the [001] direction of the InP substrate. Presently, we can further make sure that the top layer in the high-magnification image of Figure 3b is the violet phosphorus layer structure indeed. In summary, Raman, XPS and TEM characterizations confirm the successful synthesis of the atomically layered violet phosphorus on the InP substrate through the formation of InN accomplished by the plasma-assisted process. The formation mechanism is attributed to the selective reaction induced by the large difference in the variations of Gibbs free energy (ΔG) of reactions.[11]

Beyond synthesis, Hall measurements were carried out in order to elucidate carrier mobility of the atomically layered violet phosphorus for future applications. Figure 4 illustrates the relation between Hall mobility and density of carriers among different cases. All the cases were individually measured for 10 times, so that the average values could be used to make a comparison. The mobility of the pristine InP substrate was first measured as reference. Obviously, the mobility of the pristine

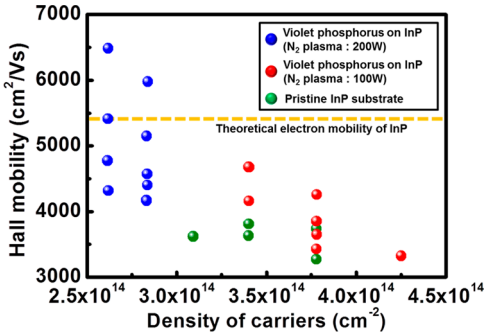

Figure 4. Plot of Hall mobility versus density of carriers.

InP substrate is ~3560 $cm^2/(V\ s)$ in average. The violet phosphorus film on the InP substrate obtained by the plasma-assisted process with the optimal condition (plasma power of 200 W, 500 °C-annealing under 400 Torr for 1.5 h) possesses a much higher Hall mobility, which is ~4940 $cm^2/(V\ s)$ in average. It should be noted that the highest mobility can be upped to ~6486 $cm^2/(V\ s)$, which is by far larger than the theoretical value of electron mobility in InP as shown in Figure 4.[19] Due to the difficulties to isolate the violet phosphorus from the InP substrate, additional tests were carried out in order to confirm that the significant enhancement of the carrier mobility is caused by the presence of the violet phosphorus. The first test was implemented by lowering the plasma power from 200 to 100 W during the synthesis. Under this condition, the mobility shows a slight improvement (~3970 $cm^2/(V\ s)$ in average); however, the results are still close to those of the pristine case as shown in Figure 4. The lower plasma power results in a lower ionization rate, implying that the concentration of nitrogen ions is too low to form a complete InN layer. Hence the continuous violet phosphorus layers could not be synthesized. Second, to further confirm the influence of the violet phosphorus on the mobility, the annealed InP substrate without the plasma immersion was also measured in order to rule out the mobility enhancement as a result of defect reduction in the InP substrate upon the annealing process (Figure S2 in the Supporting Information). Interestingly, the average mobility are below 3500 $cm^2/(V\ s)$. For the final test, we intentionally measured carrier mobility of the InP substrate after removal of violet phosphorus (Synthesis was implemented with the optimal condition mentioned above.) by Ar plasma etching with a power of 50 W for 2 min from the surface of the InP substrate. Obviously, carrier mobility is similar to that of the pristine InP substrate (Figure S2 in the Supporting Information) The Hall measurement results are summarized in Table 1 of the Supporting Information. The average Hall mobilities of all the three cases are far below that of the violet phosphorus synthesized with the optimal condition on the surface of the InP substrate. This result strongly suggests that the enhancement of carrier mobility results from the contribution of the violet phosphorus layers indeed. Nevertheless, further research should be carried out to identify the carrier mobility of the pristine material. It is noted that the violet phosphorus contributes a great enhancement of carrier mobility, but the carrier concentration just slightly decreases at the same order.

In conclusion, we have successfully expanded the plasma-assisted process previously developed for the synthesis of atomically layered violet phosphorus on the InP substrate. The synthesis condition has been optimized and the formation of

DOI: 10.1021/acsami.5b03803
ACS Appl. Mater. Interfaces 2015, 7, 13723−13727

the violet phosphorus layers was verified by multiple material analyses. The synthesis mechanism could be interpreted by the thermodynamics due to different variations of Gibbs free energy (ΔG). Most importantly, the violet phosphorus layers obtained in this work possesses high carrier mobility and high carrier concentration for device applications. This low-cost process with high compatibility has much potential for commercialization in industry.

■ ASSOCIATED CONTENT

Supporting Information

Experimental and calculation details; Figures S1 and S2; Table S1. The Supporting Information is available free of charge on the ACS Publications website at DOI: 10.1021/acsami.5b03803.

■ AUTHOR INFORMATION

Corresponding Authors

*E-mail: jhliang@ess.nthu.edu.tw.
*E-mail: ylchueh@mx.nthu.edu.tw.

Author Contributions

H.S.T. created the idea, optimized the plasma-assisted process, processed the data, finished the calculations, and wrote the manuscript. C.C.L., C.H.H., and C.(H.)O. contributed the TEM analysis. H.M. contributed the Raman analysis and the revision of manuscript. T.Y.S. contributed the XPS analysis. T.H.C. contributed the Hall measurement. J.H.L. and Y.L.C. supervised the project and contributed suggestions for the experiments.

Notes

The authors declare no competing financial interest.

■ ACKNOWLEDGMENTS

The research was supported by Ministry of Science and Technology through Grants 101-2112-M-007-015-MY3, 101-2218-E-007-009-MY3, 102-2633-M-007-002, and 102-2221-E-007-097-MY2, and National Tsing Hua University through Grant 102N2022E1. Y.L.C. greatly appreciates the use of facility at CNMM, National Tsing Hua University, through Grant 102N2744E1.

■ REFERENCES

(1) Geim, A. K.; Novoselov, K. S. The Rise of Graphene. *Nat. Mater.* **2007**, *6*, 183−191.

(2) Orlita, M.; Faugeras, C.; Plochocka, P.; Neugebauer, P.; Martinez, G.; Maude, D. K.; Barra, A. L.; Sprinkle, M.; Berger, C.; de Heer, W. A.; Potemski, M. Approaching the Dirac Point in High-Mobility Multilayer Epitaxial Graphene. *Phys. Rev. Lett.* **2008**, *101*, 267601.

(3) Nair, R. R.; Blake, P.; Grigorenko, A. N.; Novoselov, K. S.; Booth, T. J.; Stauber, T.; Peres, N. M. R.; Geim, A. K. Fine Structure Constant Defines Visual Transparency of Graphene. *Science* **2008**, *320*, 1308.

(4) Radisavljevic, B.; Radenovic, A.; Brivio, J.; Giacometti, V.; Kis, A. Single-Layer MoS_2 Transistors. *Nat. Nanotechnol.* **2011**, *6*, 147−150.

(5) Georgiou, T.; Jalil, R.; Belle, B. D.; Britnell, L.; Gorbachev, R. V.; Morozov, S. V.; Kim, Y. J.; Gholinia, A.; Haigh, S. J.; Makarovsky, O.; Eaves, L.; Ponomarenko, L. A.; Geim, A. K.; Novoselov, K. S.; Mishchenko, A. Vertical Field Effect Transistor Based on Graphene-WS_2 Heterostructures for Flexible and Transparent Electronics. *Nat. Nanotechnol.* **2013**, *8*, 100−103.

(6) Zhang, Y.; Chang, T. R.; Zhou, B.; Cui, Y. T.; Yan, H.; Liu, Z.; Schmitt, F.; Lee, J.; Moore, R.; Chen, Y.; Lin, H.; Jeng, H. T.; Mo, S. K.; Hussain, Z.; Bansil, A.; Shen, Z. X. Direct Observation of the Transition from Indirect to Direct Bandgap in Atomically Thin Epitaxial $MoSe_2$. *Nat. Nanotechnol.* **2014**, *9*, 111−115.

(7) Lee, Y. H.; Zhang, X. Q.; Zhang, W.; Chang, M. T.; Lin, C. T.; Chang, K. D.; Yu, Y. C.; Wang, T. W.; Jacob; Chang, C. S.; Li, L. J.; Lin, T. W. Synthesis of Large-Area MoS_2 Atomic Layers with Chemical Vapor Deposition. *Adv. Mater.* **2012**, *24*, 2320−2325.

(8) Li, L.; Yu, Y.; Ye, G. J.; Ge, Q.; Ou, X.; Wu, H.; Feng, D.; Chen, X. H.; Zhang, Y. Black Phosphorus Field-Effect Transistors. *Nat. Nanotechnol.* **2014**, *9*, 372−377.

(9) Xia, F.; Wang, H.; Jia, Y. Rediscovering Black Phosphorus as an Anisotropic Layered Material for Optoelectronics and Electronics. *Nat. Commun.* **2014**, *5*, 4458.

(10) Lange, S.; Schmidt, P.; Nilges, T. Au_3SnP_7@Black Phosphorus: An Easy Access to Black Phosphorus. *Inorg. Chem.* **2007**, *46*, 4028−4035.

(11) Tsai, H. S.; Lai, C. C.; Medina, H.; Lin, S. M.; Shih, Y. C.; Chen, Y. Z.; Liang, J. H.; Chueh, Y. L. Scalable Graphene Synthesised by Plasma-Assisted Selective Reaction on Silicon Carbide for Device Applications. *Nanoscale* **2014**, *6*, 13861−13869.

(12) Berger, L. I. *Semiconductor Materials*; CRC Press: Boca Raton, FL, 1996; pp 84.

(13) Thurn, Von H.; Krebs, H. Über Struktur und Eigenschaften der Halbmetalle. XXII. Die Kristallstruktur des Hittorfschen Phosphors. *Acta Crystallogr.* **1969**, *B25*, 125−135.

(14) Curry, R. Hittorf's Metallic Phosphorus of 1865. *Lateral Science*; 2012; http://lateralscience.blogspot.com/2012/07/main-menu-click-above-p-h-o-s-p-h-o-r-u.html (accessed July 8, 2012).

(15) Hittorf, W. Zur Kenntniss des Phosphors. *Ann. Phys.* **1865**, *202*, 193−228.

(16) Bhuiyan, A. G.; Hashimoto, A. Yamamoto, Indium Nitride (InN): A Review on Growth, Characterization, and Properties. *J. Appl. Phys.* **2003**, *94*, 2779−2807.

(17) Fasol, G.; Cardona, M.; Hönle, W.; von Schnering, H. G. Lattice Dynamics of Hittorf's Phosphorus and Identification of Structural Groups and Defects in Amorphous Red Phosphorus. *Solid State Commun.* **1984**, *52*, 307−310.

(18) Marcos, B.; Ibáñez, J.; Cuscó, R.; Martínez, F. L.; González-Díaz, G.; Artús, L. Lattice Recovery by Rapid Thermal Annealing in Mg^+-Implanted InP Assessed by Raman Spectroscopy. *Nucl. Instr. Meth. Phys. Res. B* **2001**, *175−177*, 252−256.

(19) Takagi, S.; Irisawa, T.; Tezuka, T.; Numata, T.; Nakaharai, S.; Hirashita, N.; Moriyama, Y.; Usuda, K.; Toyoda, E.; Dissanayake, S.; Shichijo, M.; Nakane, R.; Sugahara, S.; Takenaka, M.; Sugiyama, N. Carrier-Transport-Enhanced Channel CMOS for Improved Power Consumption and Performance. *IEEE Trans. Electron Devices* **2008**, *55*, 21−39.

DOI: 10.1021/acsami.5b03803
ACS Appl. Mater. Interfaces 2015, 7, 13723−13727